Title

PopZ identifies the new pole, and PodJ identifies the old pole during polar growth in Agrobacterium tumefaciens

Journal

Proceedings of the National Academy of Sciences of the United States of America, 112(37)

ISSN

0027-8424

Authors

Grangeon, Romain
Zupan, John R
Anderson-Furgeson, James
et al.

Publication Date

2015-09-15

DOI

10.1073/pnas.1515544112

Peer reviewed

PopZ identifies the new pole, and PodJ identifies the old pole during polar growth in *Agrobacterium tumefaciens*

Romain Grangeon, John R. Zupan, James Anderson-Furgeson, and Patricia C. Zambryski[1]

Department of Plant and Microbial Biology, University of California, Berkeley, CA 94720

Contributed by Patricia C. Zambryski, August 6, 2015 (sent for review July 1, 2015; reviewed by Vitaly Citovsky)

Agrobacterium tumefaciens **elongates by addition of peptidoglycan (PG) only at the pole created by cell division, the growth pole, whereas the opposite pole, the old pole, is inactive for PG synthesis. How *Agrobacterium* assigns and maintains pole asymmetry is not understood. Here, we investigated whether polar growth is correlated with novel pole-specific localization of proteins implicated in a variety of growth and cell division pathways. The cell cycle of *A. tumefaciens* was monitored by time-lapse and super-resolution microscopy to image the localization of *A. tumefaciens* homologs of proteins involved in cell division, PG synthesis and pole identity. FtsZ and FtsA accumulate at the growth pole during elongation, and improved imaging reveals FtsZ disappears from the growth pole and accumulates at the midcell before FtsA. The L,D-transpeptidase Atu0845 was detected mainly at the growth pole. *A. tumefaciens* specific pole-organizing protein (Pop) $PopZ_{At}$ and polar organelle development (Pod) protein $PodJ_{At}$ exhibited dynamic yet distinct behavior. $PopZ_{At}$ was found exclusively at the growing pole and quickly switches to the new growth poles of both siblings immediately after septation. $PodJ_{At}$ is initially at the old pole but then also accumulates at the growth pole as the cell cycle progresses suggesting that $PodJ_{At}$ may mediate the transition of the growth pole to an old pole. Thus, $PopZ_{At}$ is a marker for growth pole identity, whereas $PodJ_{At}$ identifies the old pole.**

Agrobacterium cell cycle | PopZ | PodJ | polar growth | bacterial cell division

The causative agent of crown gall disease in dicotylenous plants, *Agrobacterium tumefaciens*, is a free-living, soil-dwelling member of the α-proteobacteria (1). *A. tumefaciens* has been extensively studied for its ability to transfer DNA to plant cells via its *vir* type IV secretion systems (*vir*T4SS). T4SS are used by plant and animal pathogens for conjugal transfer of genetic determinants for antibiotic resistance as well as secretion of protein effectors that manipulate host cells to cause disease (2).

A. tumefaciens is a rod-shaped bacterium. The predominant model of growth for rod-shaped bacteria is elongation through addition of PG dispersed in small patches along the lateral walls of the cell envelope. This model is derived primarily from studies of *Escherichia coli* and *Bacillus subtilis* (3). Recent observation of *A. tumefaciens* and other species, however, revealed that their cells elongate by addition of PG at one or both poles depending on the organism (4, 5). Polar growth has now been documented in both Gram-positive species, including human pathogens *Mycobacterium* (6, 7) and *Streptomyces* (8, 9), and Gram negative species in the order Rhizobiales, including *Brucella* (5), *Sinorhizobium* (5), and *Agrobacterium* (4, 5, 10, 11).

Polar growth and dispersed growth are correlated with significant differences in the proteins that synthesize PG and accessory proteins involved in the spatial regulation of PG synthesis. In *E. coli*, lateral PG is synthesized by an elongasome, which includes the transpeptidase PBP2, the transglycosylase/transpeptidase PBP1a, and accessory proteins (3). Numerous elongasomes navigate the cell circumference by interaction with short filaments of the actin homolog MreB and associated structural proteins (12–14). In contrast, *A. tumefaciens* lacks homologs of most elongasome components, notably PBP2, the canonical scaffold protein MreB and accessory proteins such as MreC, MreD, RodA, and RodZ (11). Most of the machinery for PG precursor synthesis and septal PG synthesis are conserved in *A. tumefaciens*; these include carboxy- and endopeptidases, lytic transglycosylases, amidases, FtsA, three copies of FtsZ, and two copies each of PBP3, PBP1b, and FtsK (11). As A. *tumefaciens* lacks *E.coli* type cell elongation machinery, polar elongation may use a pathway mediated by a combination of coopted cell division components and novel proteins (11).

Regardless of growth mode, the poles of rod-shaped cells often constitute a distinct subcellular environment for proteins with crucial roles in motility, chemotaxis, pathogenesis, differentiation, and cell cycle progression (15). Proteins that mediate pole identity have been primarily characterized in *Caulobacter crescentus* as its two poles undergo distinct changes in morphology during its cell cycle, alternating between a motile flagellated cell and a sessile stalked cell. Two *C. crescentus* proteins, the polar organelle development (Pod) protein $PodJ_{Cc}$ and the pole-organizing protein (Pop) $PopZ_{Cc}$, localize to these dissimilar poles in a cell cycle dependent manner. In the predivisional cell, $PodJ_{Cc}$ localizes to the new pole that will become the flagellated pole opposite the stalk pole (16–18). $PopZ_{Cc}$ localization is more complex. First it localizes to the old pole at the stalk, where it forms a matrix and binds ParB to tether the chromosome (19, 20). Before division $PopZ_{Cc}$ migrates to the flagellar pole to facilitate chromosome segregation (21, 22). Homologs of $PodJ_{Cc}$ and $PopZ_{Cc}$ are encoded in Rhizobiales such as *A. tumefaciens* and *Sinorhizobium meliloti.* In *S. meliloti* (Rm1021), PodJ1 plays

Significance

Rod-shaped bacteria grow and maintain their shape by adding new material to their cell walls. Historically, most studies have focused on bacteria that grow uniformly by interspersed insertion of new material along their entire lengths. Recent work reveals another mechanism of growth from a single pole of the bacterial cell. Notably, many bacteria that use unipolar growth are important pathogens. To understand unipolar growth during the bacterial cell cycle it is critical to identify factors that may determine whether a pole is a growth pole or a non-growing pole. Here, we identify two factors, pole-organizing protein (Pop) PopZ and polar organelle development (Pod) protein PodJ that identify the growth pole and the nongrowing old pole, respectively, in the plant pathogen *Agrobacterium tumefaciens*.

Author contributions: R.G., J.R.Z., J.A.-F., and P.C.Z. designed research; R.G., J.R.Z., and J.A.-F. performed research; R.G., J.R.Z., J.A.-F., and P.C.Z. analyzed data; and R.G., J.R.Z., J.A.-F., and P.C.Z. wrote the paper.

Reviewers included: V.C., State University of New York at Stony Brook.

The authors declare no conflict of interest.

[1]To whom correspondence should be addressed. Email: zambrysk@berkeley.edu.

This article contains supporting information online at www.pnas.org/lookup/suppl/doi:10.1073/pnas.1515544112/-/DCSupplemental.

a role in maintenance of cell morphology, motility, and localization of cell-cycle regulating factors such as DivK (23).

Here, we monitor the cell cycle of *A. tumefaciens* by time-lapse microscopy. Coexpression reveals FtsZ disappears from the growth pole and appears in the Z-ring before FtsA. *A. tumefaciens* homologs ($PopZ_{At}$, $PodJ_{At}$) of polar factors $PopZ_{Cc}$ and $PodJ_{Cc}$ localize to the growth pole and old pole, respectively, an apparently opposite pattern compared with *C. crescentus*. $PopZ_{At}$ strictly localizes to growth poles, but $PodJ_{At}$ localizes to the old pole early in the cell cycle, and also localizes to the growth pole in the later stages of the cell cycle, suggesting $PodJ_{At}$ may facilitate the transition of the growth pole into an old pole just before division. Finally, we use superresolution microscopy to refine the localization of FtsA, FtsZ, $PopZ_{At}$, $PodJ_{At}$, and L,D transpeptidase Atu0845. The results reveal dynamic localization patterns of these proteins during polar growth in *A. tumefaciens*, and should provoke studies in other polar growing bacteria to identify new and old pole-specific factors.

Results

Coexpression Reveals FtsZ Localizes to the Midcell Before FtsA. Because *A. tumefaciens* lacks almost all components of the well-documented *E. coli* cell elongation machinery, we previously suggested that polar growth should be mediated by a combination of cell division components and novel proteins (11). Indeed, *A. tumefaciens* FtsA and FtsZ localized to the bacterial poles during cell elongation, and to the midcell (10, 11, 24). Here we further expand on this localization by detailed time-lapse microscopy of FtsZ (Atu2086) fused to GFP or RFP and FtsA (Atu2087) fused to GFP.

At the beginning of the cell cycle, the shortest cells with tapered ends had a single focus of FtsZ located at the growth pole (Fig. S1, 0 min). As the cell grows, the polar FtsZ focus is replaced by one or two dynamic foci in the cytoplasm (Fig. S1, 10–30 min) corresponding to the patterns previously reported in still images (10). The cytoplasmic foci migrate to the midcell by 40 min, and the midcell signal became more intense as the Z-ring forms (Fig. S1, 50–80 min). During late stages, the Z-ring constricts and appears as a dot at septation (Fig. S1, 90–100 min). Each daughter cell then will have FtsZ at the newly generated growth poles (Fig. S1, 100–110 min).

Demographs of the localization patterns in hundreds of cells suggested that FtsZ migrates to the midcell before FtsA to initiate Z-ring formation (11). Here we used time-lapse microscopy of cells coexpressing FtsZ-RFP and FtsA-GFP to directly monitor their localization during the cell cycle (Fig. 1). The localization of FtsA was unipolar during early stages of polar growth (0–20 min) and at the Z-ring during division (60–80 min). However, FtsZ migrated to the midcell when FtsA was still located to the growth pole (Fig. 1, 20 min). In the next frame, FtsA was also observed at the Z-ring (Fig. 1, 40 min). FtsA and FtsZ colocalize during the rest of the cell cycle. 3D reconstructions of SIM images of cells expressing FtsA-GFP or FtsZ-GFP show fluorescence at the midcell in a ring structure (Fig. 2*A*, Fig. 2*B*, Movie S1, and Movie S2, respectively). Thus, FtsZ and FtsA are both present at the growth pole, but FtsZ localizes to the Z-ring before FtsA.

Occasionally in one frame, we detected two Z-rings in the same cell approximately midway through the cell cycle (Fig. 2 *C* and *D* and Movie S3). In the next frame, only one Z-ring remained to mediate septation. Such double rings have been observed in *E. coli*, and are thought to represent loosely packed FtsZ filaments that form helical loops before condensation into a tight Z-ring (25). Rotation of these *A. tumefaciens* FtsZ double rings also suggests helicity (Fig. 2*D*).

$PopZ_{At}$ Localizes to the Growth Pole. The cytoplasmic $PopZ_{Cc}$ plays a crucial role during the cell cycle of *C. crescentus* (19). We used $PopZ_{Cc}$ and a BLAST search to identify $PopZ_{At}$ as a conserved hypothetical protein Atu1720. When the Atu1720 protein sequence was used as a query to search the *C. crescentus* proteome, $PopZ_{At}$ was returned as the best hit. In a Needleman–Wunsch global alignment, the Atu1720 protein sequence is 23% identical and 33% identical plus similar to $PopZ_{Cc}$ (BLOSUM62 similarity matrix). Both $PopZ_{At}$ and $PopZ_{Cc}$ contain 4 regions predicted to form α helices, and these regions are most similar (Fig. S2). $PopZ_{Cc}$ is 177 aa and $PopZ_{At}$ is 333 aa due to several insertions between predicted helices 1 and 2 (Fig. S2). In *C. crescentus*, the C-terminal 50 aa are essential for $PopZ_{Cc}$-$PopZ_{Cc}$ interaction to form a matrix that acts as a scaffold for polar factors such as ParA involved in plasmid and chromosome partitioning; this C-terminal region is 40% identical and 76% identical plus similar in *A. tumefaciens*. As $PopZ_{Cc}$-GFP is functional (22), we constructed an $PopZ_{At}$-GFP fusion to test for $PopZ_{At}$ localization.

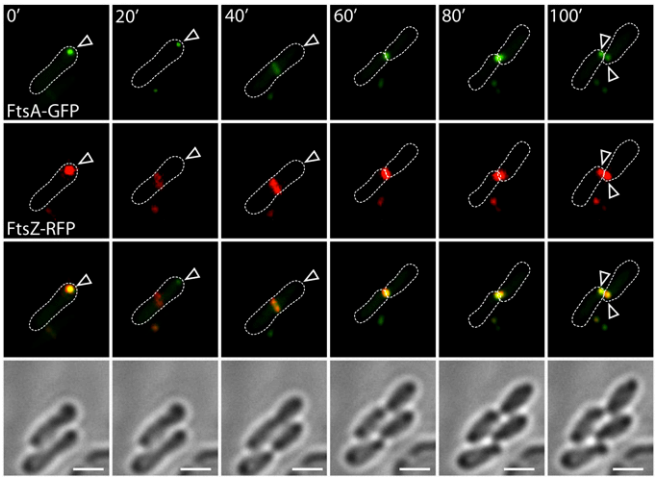

Fig. 1. Time-lapse microscopy of *A. tumefaciens* coexpressing FtsZ-RFP and FtsA-GFP. First row, FtsA-GFP. Second row, FtsZ-RFP. Third row, overlay of GFP and RFP. Fourth row, brightfield. The second frame (20 min) shows FtsZ beginning to form the Z-ring, when FtsA is still located at the growth pole. Cell outlines shown as dotted white lines. Arrowheads indicate growth poles. (Scale bar = 1 μm.)

$PopZ_{At}$ exhibits tightly controlled dynamic spatial and temporal localization during the cell cycle. Unlike *C. crescentus*, $PopZ_{At}$ was found exclusively at the growth pole (Fig. 3*A* and Movie S4). Demographic assessment of $PopZ_{At}$ localization in hundreds of cells confirms unipolar localization Fig. 3*C*). An interesting feature of the $PopZ_{At}$ pattern was its rapid relocalization at cell division (Fig. 3*A*). $PopZ_{At}$ localizes at the growth pole until the very end of the cell cycle (80 min) and then relocalizes to the new growth poles (100 min) as soon as daughter cells separate. Expression of $PopZ_{Cc}$ in *E.coli* exhibits polar localization (19). In contrast, heterologous expression of $PopZ_{At}$ in *E. coli* results in diffuse localization (Fig. S3*A*) suggesting that polar accumulation of $PopZ_{At}$ in *A. tumefaciens* does not occur by a mechanism that is intrinsic to $PopZ_{At}$ itself, but instead may require accessory species specific factors.

$PodJ_{At}$ Localizes to the Old Pole and to the Growth Pole Late in the Cell Cycle. Several aspects of polar morphogenesis in *C. crescentus* require $PodJ_{Cc}$ (16, 17, 26–28). We used $PodJ_{Cc}$ and a BLAST search to identify $PodJ_{At}$ as a conserved hypothetical protein Atu0499. When Atu0499 was used as a query to search the *C. crescentus* proteome, $PodJ_{Cc}$ was returned as the best hit. In a Needleman–Wunsch global alignment, the Atu0499 protein sequence is 23% identical to $PodJ_{Cc}$ (BLOSUM62 similarity matrix) and 35% identical plus similar. Atu0499 and the *S. meliloti* (SM11) PodJ are also reciprocal best BLAST hits, and are 47.6% identical and 62.5% identical plus similar. $PodJ_{At}$ is longer (1,248 aa) than $PodJ_{Cc}$ (974 aa) (Fig. S4). According to the consensus prediction of membrane protein topology program TOPCONS (topcons.cbr.su.se) $PodJ_{At}$ and $PodJ_{Cc}$ share a topology profile with most of the protein in the cytoplasm (641 aa in *C. crescentus* and 830 aa in *A. tumefaciens*), followed by a transmembrane domain. The cytoplasmic

MICROBIOLOGY

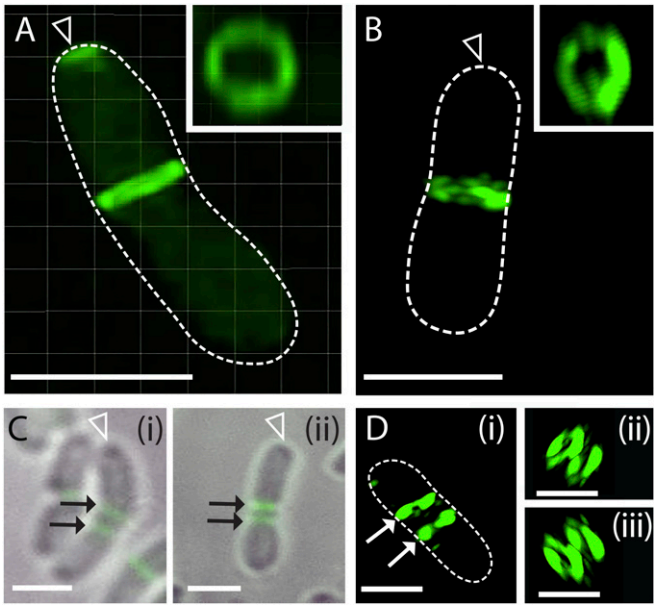

Fig. 2. FtsA and FtsZ in Z-rings. (*A*) 3D SIM of FtsA-GFP at the growth pole, and at the midcell where it forms a ring (*Inset*). (*B*) 3D-SIM of FtsZ-GFP shows a typical Z-ring in side view and inset. (*C*) Occasionally double FtsZ-rings were observed by deconvolution fluorescence microscopy (black arrows); *i* and *ii* show different cells with double Z-rings. (*D*) 3D-SIM of a double Z-ring (white arrows); *i*, *ii*, and *iii* are different views of the same Z-ring (s). Cell outlines shown as dotted white lines. All images taken in cells with wide Z-rings before contraction at division. Arrowheads, growth poles. (Scale bars = 1 μm.)

domain of both proteins contains several predicted coiled-coil regions (refs. 28 and 29, Fig. S4, respectively). The periplasmic C-terminal domains (323 aa *C. crescentus* and 397 aa in *A. tumefaciens*) carry Sel1-like repeats and a PG binding site (refs. 28 and 29, Fig. S4, respectively).

To determine whether localization of $PodJ_{At}$ suggests a role in pole identity, we fused GFP to the cytoplasmic N terminus of $PodJ_{At}$ and examined its subcellular localization during the cell cycle (Fig. 3*B* and Movie S5). We fused GFP to the N terminus of the cytoplasmic domain of PodJ as a N-terminal fusion to PodJ is functional in *C. crescentus* (17) and *S. meliloti* (23). Note, a C-terminal GFP fusion would likely interfere with the periplasmic PG binding domain, which is at the very C terminus of PodJ. At the beginning of the cell cycle, $PodJ_{At}$ is unipolar and located strictly at the old pole (Fig. 3*B*, 0–20 min). Twenty minutes later $PodJ_{At}$ was still at the old pole, but also exhibited a very weak labeling of the growth pole (Fig. 3*B*, 40 min). Later $PodJ_{At}$ was completely bipolar (Fig. 3*B*, 60 min), and remained bipolar during septation (Fig. 3*B*, 80 min, Fig. 4*A*) resulting in an old pole-labeling pattern after cell division in the two daughter cells (Fig. 3*B*, 100 min). $PodJ_{At}$ accumulates at the growth pole (60 min) just before these poles have reached their final length (80 min); during this time frame this pole must transition (red triangle, Fig. 3*D*) from active growth to a nongrowing old pole. Demographic analyses confirm $PodJ_{At}$ localizes to old poles in shorter growing cells, and to both poles in longer cells (later in the cell cycle) (Fig. 3*D*). *S. meliloti* PodJ1 localizes to the "newer" pole just before cell division and persists in only one daughter cell at the old pole (23); thus, there is no bipolar localization of PodJ1 in *S. meliloti*. When we expressed GFP-$PodJ_{At}$ in *E. coli* it localized at the poles but also at the midcell (Fig. S3*B*) suggesting it can localize to heterologous poles.

To further investigate the temporal relationship between $PodJ_{At}$ and $PopZ_{At}$ localization during the cell cycle, we coexpressed RFP-$PodJ_{At}$ and $PopZ_{At}$-GFP and focused on the late stages of the cell cycle, immediately before and post cell division (Fig. 4*A*). At the end of the cell cycle, $PodJ_{At}$ was located at both poles, whereas $PopZ_{At}$ was only at the growth pole (Fig. 4*A*, 0 min). Just after cell division, $PopZ_{At}$ rapidly disappears from what is now an old pole and appears at the newly created growth poles at the division site

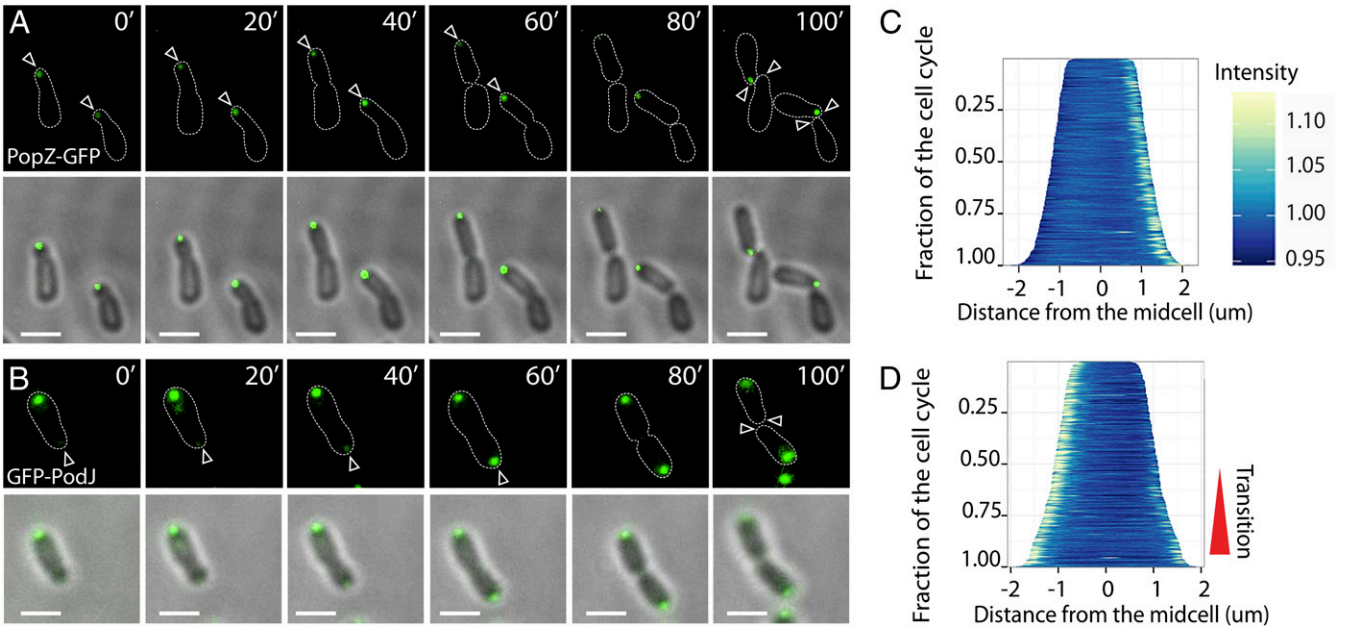

Fig. 3. $PopZ_{At}$ and $PodJ_{At}$ localization. Time-lapse microscopy of *A. tumefaciens* expressing $PopZ_{At}$-GFP (*A*) or GFP-$PodJ_{At}$ (*B*) shows $PopZ_{At}$ localizes to new growth poles, whereas $PodJ_{At}$ localizes to the old pole during the early part of the cell cycle and then also to the growth pole later in the cell cycle. Fluorescence images (with cell outlines as white dashed lines) are shown above overlays of fluorescence and brightfield images. Arrowheads indicate growth poles. (Scale bar = 1 μm.) (*C*) Demograph of cells expressing $PopZ_{At}$-GFP (n = 500). (*D*) Demograph of cells expressing GFP-$PodJ_{At}$ (n = 400). Demographs are oriented with the growth pole on the right, using FM4-64 old pole-specific labeling (10) as a reference. Red triangle indicates the predicted growth pole–old pole transition marked by accumulation of PodJ.

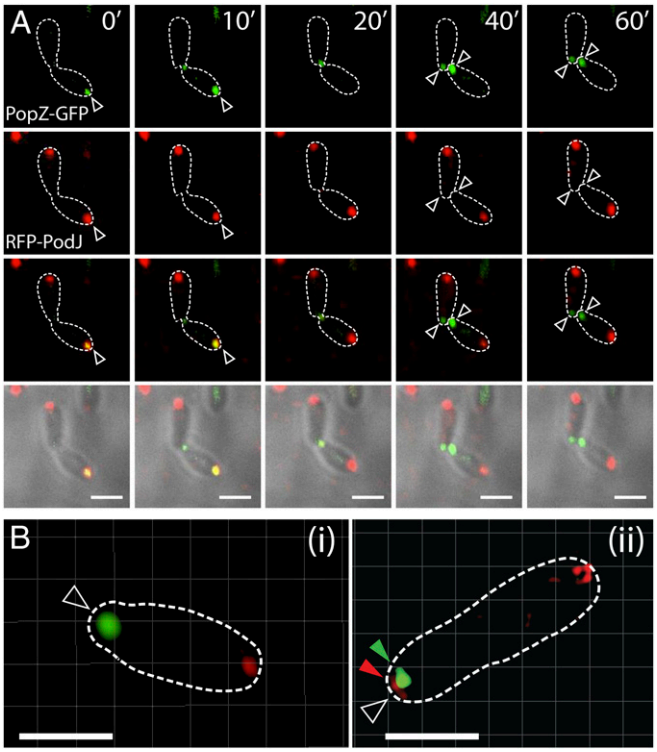

Fig. 4. Simultaneous monitoring of $PopZ_{At}$ and $PodJ_{At}$ during the cell cycle. Time-lapse microscopy of *A. tumefaciens* coexpressing $PopZ_{At}$-GFP and RFP-$PodJ_{At}$. (*A*) First row, $PopZ_{At}$-GFP. Second row, RFP-$PodJ_{At}$. Third row, simultaneous imaging of $PopZ_{At}$-GFP and RFP-$PodJ_{At}$. Cell outlines are indicated by white dotted lines in fluorescence images. Fourth row, fluorescence of $PopZ_{At}$-GFP and RFP-$PodJ_{At}$ coexpression, overlaid on brightfield images. (*B*) Simultaneous imaging of $PopZ_{At}$-GFP and RFP-$PodJ_{At}$ by 3D-SIM. $PopZ_{At}$-GFP localizes to the growth pole and GFP-$PodJ_{At}$ to the old pole during the early polar growth phase of the cell cycle (*i*). When the cell is longer and close to division, $PodJ_{At}$ also localizes to the extreme tip of the growth pole (red arrow, *ii*), whereas $PopZ_{At}$ is subpolar (green arrow, *ii*). Arrowheads indicate growth poles. (Scale bar = 1 μm.)

(Fig. 4*A*, 10 min and 20 min). Cell division creates two daughter cells with a single focus of $PodJ_{At}$ at the old pole of each cell and a focus of $PopZ_{At}$ at each of the new poles (Fig. *4A*, 40 min). Thus, the growth pole-old pole transition includes the removal of $PopZ_{At}$ as well as the accumulation of $PodJ_{At}$.

Widefield fluorescence microscopy suggests that $PopZ_{At}$ and $PodJ_{At}$ colocalize at the growth pole later in the cell cycle (Fig. 4*A*, 0 and 20 min). The higher resolution afforded by SIM, however, distinguishes each protein into a slightly different region of the pole (Fig. 4*B*). $PodJ_{At}$ is located at the extreme cell tip, whereas $PopZ_{At}$ is located at an adjacent, slightly subpolar site (Fig. 4*B*, green and red arrowheads). The slight difference in polar localization is consistent with the fact that $PodJ_{At}$ is likely a monotypic inner membrane protein and $PopZ_{At}$ is cytoplasmic.

Time-Lapse Microscopy of L,D Transpeptidase Atu0845. *A. tumefaciens* and other members of the Rhizobiales contain an unusual abundance of putative L,D-transpeptidase (LDT) proteins (11). Unlike the D,D-transpeptidases (DDTs) (e.g., PBP3) that form 4,3-cross-links between D-alanine and m-Dap of two PG stem peptides, LDTs catalyze 3,3-cross-links between two m-Dap residues and are insensitive to most penicillins (11, 30). More than 50% of the peptide cross-links in *A. tumefaciens* and the related *S. meliloti* are 3,3-cross-links (5) compared with only 10% in *E. coli* (31).

We recently showed that Atu0845, an LDT specific to the Rhizobiales, localizes strongly to the growth pole in a broad cap (versus discrete foci as for FtsA/Z), and labeling with fluorescent PG substrates reveals a gradient of weaker localization distal to the pole (11). This pattern of localization is expected for an essential polar PG synthesis factor. As DDTs and LDTs function in the periplasm we fused Atu0845 at its C terminus to superfolding GFP to allow its detection. We monitored Atu0845-GFP for 180 min, one complete cell cycle and up to just before the second division (Fig. 5*A* and Movie S6). Atu0845 localized to the growth pole during the entire cell cycle (zero to ∼90 min), and also showed septal labeling during division (60-80 min). Late in the cell cycle labeling at the growth pole decreases as the new pole reaches its full length and transitions into an old pole. Following division, labeling is more intense at the new poles in daughter cells, but remains weak at the old pole (120–180 min). The weak localization of Atu0845 at the old pole is inherited from the previous division cycle, when the old pole was a growth pole. As no detectable PG synthesis occurs in old poles (11) Atu0845-GFP must be relatively stable, albeit locally inactive.

We also imaged cells expressing Atu0845-sfGFP by 3D SIM (Fig. 5*B* and Movie S7). Atu0845 localization appears as an arc at the growth pole (Fig. 5 *B* and *C* and Movie S7). The cell outline is shown by staining with the lipophilic membrane dye FM 4–64, which does not stain the growth pole (10). The weak localization of Atu0845-sfGFP to the old pole (arrow, Fig. 5*B*) is likely a remnant of its localization during polar growth in the previous cell cycle (see supplemental figure 5 from ref. 11).

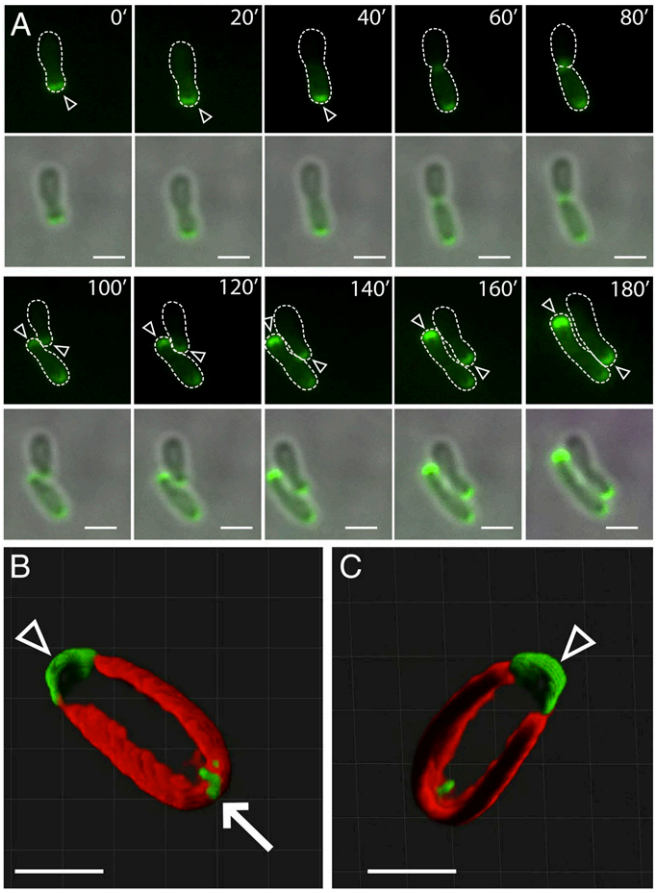

Fig. 5. L,D-transpeptidase Atu0845 primarily localizes to the new pole. (*A*) Time-lapse microscopy of *A. tumefaciens* expressing Atu0845-sfGFP. Top row and third row, fluorescence images. Cell outlines shown as dotted white lines. Second row and fourth row, overlay of fluorescence and brightfield images. (*B* and *C*) 3D SIM of Atu0845-GFP. Atu0845 appears strongly at the growth pole, and weakly at the old pole. Cell polarity is determined by FM4-64 preferential labeling of the old pole versus the growth pole (10). White arrow shows Atu0845 closely associated with the membrane (*B*). Arrowheads indicate growth poles. (Scale bar = 1 μm.)

MICROBIOLOGY

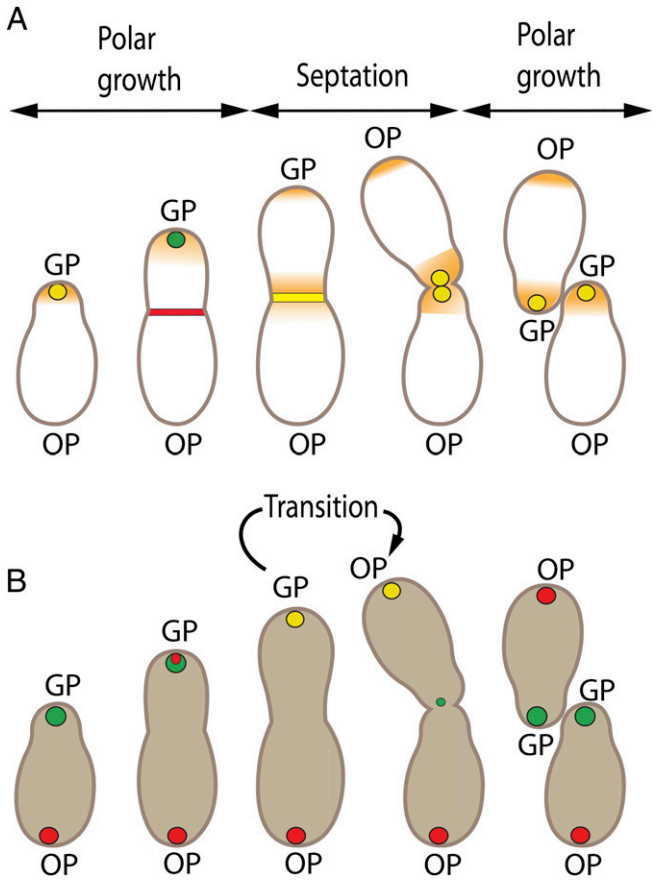

Fig. 6. Summary of FtsA, FtsZ, $PopZ_{At}$, $PodJ_{At}$, and Atu0845 localization during the *A. tumefaciens* cell cycle. (*A*) FtsA and FtsZ colocalize (yellow) at the beginning of the cell cycle. FtsZ (red) leaves the growth pole (GP) to begin to form the Z-ring before FtsA (green). LDT Atu0845 localizes (brown shading) to regions of active PG synthesis at the GP and later at the midcell. (*B*) Localization of $PopZ_{At}$ (green) and $PodJ_{At}$ (red). Colocalization indicated by (yellow) and curved arrow indicates the transition of the GP into an old pole (OP). See text for details.

Discussion

Here we monitored key proteins involved in cell division, PG synthesis, and pole identity to identify factors participating in polar growth in *A. tumefaciens*. Overall, the dynamic localization of the *A. tumefaciens* proteins exhibits striking differences from that reported for their homologs in other model systems such as *E. coli* or *C. crescentus*. Besides spatial localization to the new pole, old pole, or midcell, the temporal patterns of localization of *A. tumefaciens* proteins suggest a distinct time frame when the growth pole transitions into an old pole.

In *E. coli* and *B. subtilis*, the cell division protein FtsZ arrives at the midcell along with FtsA (32–34); these proteins do not exhibit any other distinct localizations during the cell cycle of these organisms. However, in *A. tumefaciens* FtsZ and FtsA localize to the growth pole during almost half of the cell cycle, and then migrate to the midcell for division (10, 11, 24). Here, timelapse observations reveal FtsZ disappears from the growth pole to form the midcell Z-ring significantly (~20 min) before FtsA; in *C. crescentus* FtsZ also arrives at the midcell before FtsA (35).

$PopZ_{Cc}$ exhibits dynamic behavior localizing to both stalked and flagellated poles (19–22). In contrast, $PopZ_{At}$ unambiguously marks the growth pole during the entire cell cycle, from the beginning of polar growth in newly generated daughter cells to just before cell division, and SIM reveals $PopZ_{At}$ as a sharp focus at the pole tip. The rapid disappearance of $PopZ_{At}$ from the growth pole and its reappearance in the daughter cells immediately following septation suggests that $PopZ_{At}$ may also play a role during septation.

$PodJ_{Cc}$ is an integral membrane protein containing a periplasmic PG-binding domain (28, 36). $PodJ_{Cc}$ is required for motility, flagellar release, holdfast formation, pili production and general pole identity (16–18, 27). In *S. meliloti*, deletion of *podJ1* decreased flagellar motility, exopolysaccharide production, cell envelope integrity, cell division, and altered cell morphology (23). Here we show $PodJ_{At}$ always localizes to the old pole during polar growth. Interestingly, $PodJ_{At}$ starts to accumulate at the new pole during the later stages of the cell cycle (40–60 min), and remains at this pole post cell division thereby marking the newest old pole. This latter localization pattern suggests the new pole undergoes a transition to become an old pole, and that $PodJ_{At}$ is a marker for this transition. What determines old pole identity? At least three changes must occur, PG synthesis and cross-linking slow down, the PG must adopt a specific and stable curvature, and membranes must mature as old poles differentially label with FM4-64 (10).

Fig. 6 highlights the transitions in localization of different landmark proteins during the *A. tumefaciens* cell cycle. Coexpressed FtsA-GFP and FtsZ-RFP colocalize during most of the cell cycle. FtsZ leaves the growth pole (GP) to begin to form the Z-ring before FtsA. Post cell division, FtsA and FtsZ again colocalize at the new GPs. LDT Atu0845 localizes to regions of active PG synthesis at the GP and later at the midcell. Coexpressed $PopZ_{At}$-GFP and RFP-$PodJ_{At}$ have distinct localizations during polar growth where $PopZ_{At}$ identifies the GP, and $PodJ_{At}$ identifies the old pole (OP). $PopZ_{At}$ and $PopJ_{At}$ colocalize during a transition stage where the GP becomes an OP likely under the influence of $PodJ_{At}$. During this transition $PopZ_{At}$ begins to relocate to the septum, and post division $PopZ_{At}$ uniquely marks new GPs in sibling cells. $PopZ_{At}$ and $PodJ_{At}$ are significantly longer proteins than their *C. crescentus* counterparts; these additional domains may play a role in their distinct localizations in *A. tumefaciens.*

Many exciting questions remain to be addressed to further understand unipolar bacterial growth (37). What are the exact mechanisms underlying the growth pole-old pole transition? Besides $PodJ_{At}$, what additional factors are involved? *A. tumefaciens* has four genetic elements (two large chromosomes and two large plasmids). How does chromosome segregation occur during polar growth? An early study suggested these genetic elements localize to a single pole in short growing cells (38); however growth poles and old poles were not distinguished. How does a tapered growth pole increase its diameter to establish normal cell width? Is there an advantage for an old pole to remain an old pole forever? The *A. tumefaciens* genome does not encode obvious homologs of scaffolding proteins such as MreB, RodA, and RodZ (39); does *A. tumefaciens* require scaffold proteins and what might they be? These processes are likely coordinated with the specification of growth and old poles reflected by the cell-cycle-specific changes in protein localization described here.

Materials and Methods

Strains and Plasmids. Strains and plasmids are listed in Table S1. *A. tumefaciens* C58 containing pTiC58 was transformed with the plasmids described and cultured overnight at 28 °C in liquid Luria Broth (LB) media supplemented with appropriate antibiotics. To obtain exponential growth and induce fusion protein expression, cultures were diluted to 10^8 cells per mL in LB containing 10 mM isopropyl-β-D-thiogalactopyranoside (IPTG) and antibiotics and grown for 4–5 h at 28 °C. Fluorescent protein fusions were expressed at low levels from the low copy number pSRK plasmid where the IPTG inducible promoter is tightly regulated (40); FtsZ-GFP reaches ~10% of native levels (10), and FtsA-GFP reaches ~12.5% of native levels (11).

Microscopy.

Time lapse imaging. We used the CellASIC ONIX Microfluidic Platform and B04 plates. Before loading bacteria, the plate was flushed with LB containing 10 mM IPTG for 30 min at 4 psi. Cells (100 μL at 3×10^9 cells per mL) were loaded into the plate and continuously perfused with LB containing 10 mM IPTG at room temperature. Images were acquired every 10 min for 240 min on an Applied Precision Delta Vision Elite (APDVE) deconvolution microscope.

Standard fluorescent microscopy. Slides were prepared by first covering a microscope slide with a thin (~150–200 nm) layer of 1.5% agarose in PBS (pH 7.4). Once solidified, the agarose was trimmed to the size of a cover- slip. Bacteria were resuspended at 3×10^9 cells per mL, and 1 μL was placed on top of each agarose pad, covered with a coverslip, and sealed with nail polish. Images were taken with the APDVE deconvolution microscope and processed using Fiji/ImageJ (version 1.49t; fiji.sc). Demographs were constructed by first measuring fluorescence intensity profiles in Fiji and then processing the data in R (version 3.0.2; R Foundation for Statistical Computing; www.r-project.org) using a script (11) designed to sort cells by length and normalize intensity profiles by each cell's average fluorescence. Demographs were generated in R using the ggplot2 package (version 0.9.3.1; Hadley Wickham, Department of Statistics, Rice University; ggplot2.org).

Structured illumination microscopy (SIM). Superresolution images were captured using a Zeiss Elyra PS.1 SIM equipped with a Zeiss PlanApochromat 100x/1.46 oil immersion objective lens and a pco.edge sCMOS camera with a 1.6× tube lens. GFP fluorescence was stimulated with 488-nm laser excitation, and RFP or FM4-64 fluorescence with 561-nm laser excitation. The lateral pixel size, Dx and Dy, was 41 nm in the recorded images. Z-stacks were acquired by capturing 20 slices of 0.1-μm step size. 3D-SIM images were reconstructed using ZEN 2012 black edition (Carl Zeiss) and processed with Imaris 8.1 (Bitplane scientific).

ACKNOWLEDGMENTS. We thank Steven Ruzin and Denise Schichnes [Biological Imaging Facility, (BIF) University of California, Berkeley] for assistance with microscopy. Research was supported by National Science Foundation Grant MCB-1243360 (to P.C.Z.). We thank the National Institutes of Health S10 program (1S0OD018136-01) for funds for BIF to purchase the Zeiss Elyra PS.1 microscope.

1. Zupan J, Muth TR, Draper O, Zambryski P (2000) The transfer of DNA from *agrobacterium tumefaciens* into plants: A feast of fundamental insights. *Plant J* 23(1): 11–28.
2. Trokter M, Felisberto-Rodrigues C, Christie PJ, Waksman G (2014) Recent advances in the structural and molecular biology of type IV secretion systems. *Curr Opin Struct Biol* 27:16–23.
3. den Blaauwen T, de Pedro MA, Nguyen-Distèche M, Ayala JA (2008) Morphogenesis of rod-shaped sacculi. *FEMS Microbiol Rev* 32(2):321–344.
4. Brown PJB, Kysela DT, Brun YV (2011) Polarity and the diversity of growth mechanisms in bacteria. *Semin Cell Dev Biol* 22(8):790–798.
5. Brown PJB, et al. (2012) Polar growth in the Alphaproteobacterial order Rhizobiales. *Proc Natl Acad Sci USA* 109(5):1697–1701.
6. Thanky NR, Young DB, Robertson BD (2007) Unusual features of the cell cycle in mycobacteria: Polar-restricted growth and the snapping-model of cell division. *Tuberculosis (Edinb)* 87(3):231–236.
7. Meniche X, et al. (2014) Subpolar addition of new cell wall is directed by DivIVA in mycobacteria. *Proc Natl Acad Sci USA* 111(31):E3243–E3251.
8. Braña AF, Manzanal M-B, Hardisson C (1982) Mode of cell wall growth of *Streptomyces antibioticus*. *FEMS Microbiol Lett* 13(3):231–235.
9. Miguélez EM, Martín C, Manzanal MB, Hardisson C (1992) Growth and morphogenesis in *Streptomyces*. *FEMS Microbiol Lett* 100(1-3):351–359.
10. Zupan JR, Cameron TA, Anderson-Furgeson J, Zambryski PC (2013) Dynamic FtsA and FtsZ localization and outer membrane alterations during polar growth and cell division in *Agrobacterium tumefaciens*. *Proc Natl Acad Sci USA* 110(22):9060–9065.
11. Cameron TA, Anderson-Furgeson J, Zupan JR, Zik JJ, Zambryski PC (2014) Peptidoglycan synthesis machinery in *Agrobacterium tumefaciens* during unipolar growth and cell division. *MBio* 5(3):e01219–14.
12. van Teeffelen S, et al. (2011) The bacterial actin MreB rotates, and rotation depends on cell-wall assembly. *Proc Natl Acad Sci USA* 108(38):15822–15827.
13. Garner EC, et al. (2011) Coupled, circumferential motions of the cell wall synthesis machinery and MreB filaments in *B. subtilis*. *Science* 333(6039):222–225.
14. Domínguez-Escobar J, et al. (2011) Processive movement of MreB-associated cell wall biosynthetic complexes in bacteria. *Science* 333(6039):225–228.
15. Laloux G, Jacobs-Wagner C (2014) How do bacteria localize proteins to the cell pole? *J Cell Sci* 127(1):11–19.
16. Hinz AJ, Larson DE, Smith CS, Brun YV (2003) The *Caulobacter crescentus* polar organelle development protein PodJ is differentially localized and is required for polar targeting of the PleC development regulator. *Mol Microbiol* 47(4):929–941.
17. Viollier PH, Sternheim N, Shapiro L (2002) Identification of a localization factor for the polar positioning of bacterial structural and regulatory proteins. *Proc Natl Acad Sci USA* 99(21):13831–13836.
18. Chen JC, et al. (2006) Cytokinesis signals truncation of the PodJ polarity factor by a cell cycle-regulated protease. *EMBO J* 25(2):377–386.
19. Bowman GR, et al. (2008) A polymeric protein anchors the chromosomal origin/ParB complex at a bacterial cell pole. *Cell* 134(6):945–955.
20. Ebersbach G, Briegel A, Jensen GJ, Jacobs-Wagner C (2008) A self-associating protein critical for chromosome attachment, division, and polar organization in *caulobacter*. *Cell* 134(6):956–968.
21. Ptacin JL, et al. (2014) Bacterial scaffold directs pole-specific centromere segregation. *Proc Natl Acad Sci USA* 111(19):E2046–E2055.
22. Laloux G, Jacobs-Wagner C (2013) Spatiotemporal control of PopZ localization through cell cycle-coupled multimerization. *J Cell Biol* 201(6):827–841.
23. Fields AT, et al. (2012) The conserved polarity factor podJ1 impacts multiple cell envelope-associated functions in *Sinorhizobium meliloti*. *Mol Microbiol* 84(5):892–920.
24. Ma X, et al. (1997) Interactions between heterologous FtsA and FtsZ proteins at the FtsZ ring. *J Bacteriol* 179(21):6788–6797.
25. Fu G, et al. (2010) In vivo structure of the *E. coli* FtsZ-ring revealed by photoactivated localization microscopy (PALM). *PLoS One* 5(9):e12682.
26. Wang SP, Sharma PL, Schoenlein PV, Ely B (1993) A histidine protein kinase is involved in polar organelle development in *Caulobacter crescentus*. *Proc Natl Acad Sci USA* 90(2):630–634.
27. Smith CS, Hinz A, Bodenmiller D, Larson DE, Brun YV (2003) Identification of genes required for synthesis of the adhesive holdfast in *Caulobacter crescentus*. *J Bacteriol* 185(4):1432–1442.
28. Lawler ML, Larson DE, Hinz AJ, Klein D, Brun YV (2006) Dissection of functional domains of the polar localization factor PodJ in *Caulobacter crescentus*. *Mol Microbiol* 59(1):301–316.
29. Curtis PD, et al. (2012) The scaffolding and signalling functions of a localization factor impact polar development. *Mol Microbiol* 84(4):712–735.
30. Magnet S, Dubost L, Marie A, Arthur M, Gutmann L (2008) Identification of the L,D-transpeptidases for peptidoglycan cross-linking in *Escherichia coli*. *J Bacteriol* 190(13):4782–4785.
31. Glauner B, Höltje JV, Schwarz U (1988) The composition of the murein of *Escherichia coli*. *J Biol Chem* 263(21):10088–10095.
32. Rueda S, Vicente M, Mingorance J (2003) Concentration and assembly of the division ring proteins FtsZ, FtsA, and ZipA during the Escherichia coli cell cycle. *J Bacteriol* 185(11):3344–3351.
33. Aarsman MEG, et al. (2005) Maturation of the *Escherichia coli* divisome occurs in two steps. *Mol Microbiol* 55(6):1631–1645.
34. Jensen SO, Thompson LS, Harry EJ (2005) Cell division in *Bacillus subtilis*: FtsZ and FtsA association is Z-ring independent, and FtsA is required for efficient midcell Z-Ring assembly. *J Bacteriol* 187(18):6536–6544.
35. Goley ED, et al. (2011) Assembly of the *Caulobacter* cell division machine. *Mol Microbiol* 80(6):1680–1698.
36. Treuner-Lange A, Søgaard-Andersen L (2014) Regulation of cell polarity in bacteria. *J Cell Biol* 206(1):7–17.
37. Cameron TA, Zupan JR, Zambryski PC (2015) The essential features and modes of bacterial polar growth. *Trends Microbiol* 23(6):347–353.
38. Kahng LS, Shapiro L (2003) Polar localization of replicon origins in the multipartite genomes of *Agrobacterium tumefaciens* and *Sinorhizobium meliloti*. *J Bacteriol* 185(11):3384–3391.
39. Bendezú FO, Hale CA, Bernhardt TG, de Boer PAJ (2009) RodZ (YfgA) is required for proper assembly of the MreB actin cytoskeleton and cell shape in *E. coli*. *EMBO J* 28(3):193–204.
40. Khan SR, Gaines J, Roop RM, 2nd, Farrand SK (2008) Broad-host-range expression vectors with tightly regulated promoters and their use to examine the influence of TraR and TraM expression on Ti plasmid quorum sensing. *Appl Environ Microbiol* 74(16):5053–5062.
41. Zupan J, Hackworth CA, Aguilar J, Ward D, Zambryski P (2007) VirB1* promotes T-pilus formation in the vir-Type IV secretion system of Agrobacterium tumefaciens. *J Bacteriol* 189(18):6551–6563.
42. Lupas A, Van Dyke M, Stock J (1991) Predicting coiled coils from protein sequences. *Science* 252(5009):1162–1164.